Washington University School of Medicine
Digital Commons@Becker

Open Access Publications

1-5-2004

Role of the hydrophobic domain in targeting caveolin-1 to lipid droplets

Anne G. Ostermeyer
State University of New York at Stony Brook

Lynne T. Ramcharan
State University of New York at Stony Brook

Youchun Zeng
Washington University School of Medicine in St. Louis

Douglas M. Lublin
Washington University School of Medicine in St. Louis

Deborah A. Brown
State University of New York at Stony Brook

Follow this and additional works at: http://digitalcommons.wustl.edu/open_access_pubs

 Part of the Medicine and Health Sciences Commons

Recommended Citation
Ostermeyer, Anne G.; Ramcharan, Lynne T.; Zeng, Youchun; Lublin, Douglas M.; and Brown, Deborah A., ,"Role of the hydrophobic domain in targeting caveolin-1 to lipid droplets." The Journal of Cell Biology.164,1. 69-78. (2004).
http://digitalcommons.wustl.edu/open_access_pubs/623

This Open Access Publication is brought to you for free and open access by Digital Commons@Becker. It has been accepted for inclusion in Open Access Publications by an authorized administrator of Digital Commons@Becker. For more information, please contact engeszer@wustl.edu.

Published January 5, 2004

JCB Article

Role of the hydrophobic domain in targeting caveolin-1 to lipid droplets

Anne G. Ostermeyer,[1] Lynne T. Ramcharan,[1] Youchun Zeng,[2] Douglas M. Lublin,[2] and Deborah A. Brown[1]

[1]Department of Biochemistry and Cell Biology, State University of New York at Stony Brook, Stony Brook, NY 11794
[2]Department of Pathology, Washington University School of Medicine, St. Louis, MO 63110

Although caveolins normally reside in caveolae, they can accumulate on the surface of cytoplasmic lipid droplets (LDs). Here, we first provided support for our model that overaccumulation of caveolins in the endoplasmic reticulum (ER) diverts the proteins to nascent LDs budding from the ER. Next, we found that a mutant H-Ras, present on the cytoplasmic surface of the ER but lacking a hydrophobic peptide domain, did not accumulate on LDs. We used the fact that wild-type caveolin-1 accumulates in LDs after brefeldin A treatment or when linked to an ER retrieval motif to search for mutants defective in LD targeting. The hydrophobic domain, but no specific sequence therein, was required for LD targeting of caveolin-1. Certain Leu insertions blocked LD targeting, independently of hydrophobic domain length, but dependent on their position in the domain. We propose that proper packing of putative hydrophobic helices may be required for LD targeting of caveolin-1.

Introduction

Lipid droplets (LDs), which are present in the cytoplasm of most eukaryotic cells, consist of triacylglyceride and steryl ester–rich cores surrounded by phospholipid monolayers (Londos et al., 1999; Zweytick et al., 2000; Murphy, 2001). LDs are thought to form by budding from the ER through an unusual and poorly characterized mechanism. First, neutral lipids (synthesized in the ER membrane) accumulate in the center of the bilayer and form disks. Next, the disks bulge into the cytoplasm as they enlarge and eventually bud from the ER as LDs, acquiring ER-derived phospholipid monolayers in the process.

Although no proteins are known to reside in the hydrophobic LD core, several proteins are targeted to the LD surface. Little is known about the function of most of these. Among the best understood are the oleosins, which are abundant proteins in certain plants seeds that prevent oil body (plant LD) coalescence during desiccation (Huang, 1992; Murphy, 2001). Oleosins are targeted to oil bodies when expressed in animal cells, showing that targeting mechanisms are conserved between kingdoms (Hope et al., 2002). Caleosins, which are related to oleosins, are Ca^{2+}-binding LD proteins of unknown function in plants and fungi (Chen et al., 1999; Naested et al., 2000). The best characterized LD proteins in animal cells are the perilipins, which coat the LD surface in adipocytes and steroidogenic cells. Londos et al. (1999) have shown that the phosphorylation state of perilipins regulates the access of hormone-sensitive lipase to the LD surface, and that this regulates mobilization of lipid stores (Tansey et al., 2003). Consistent with this model, regulation of lipid metabolism in adipocytes is perturbed in perilipin-deficient mice (Martinez-Botas et al., 2000; Tansey et al., 2001). A related LD protein, adipocyte differentiation related protein (ADRP) or adipophilin, is widely distributed in mammalian cells (Brasaemle et al., 1997b). The core proteins of hepatitis C virus (HCV) and the related GB virus-B (GBV-B) are also targeted at least partially to LDs (Barba et al., 1997; Hope et al., 2002). Other proteins, such as hormone-sensitive lipase in adipocytes, can associate with LDs transiently (Egan et al., 1992).

LD proteins fall into two structural classes. The first class includes perilipins and ADRP. Perilipins have no long hydrophobic domains, are made on free polysomes (Brasaemle et al., 1997a), and are probably targeted directly from the cytosol to the LD surface. It has not been possible to identify simple discrete LD targeting motifs in either perilipins or ADRP

Address correspondence to D.A. Brown, Department of Biochemistry and Cell Biology, State University of New York at Stony Brook, Stony Brook, NY 11794-5215. Tel.: (631) 632-8563. Fax: (631) 632-8575. email: deborah.brown@sunysb.edu

Key words: secondary protein structure; caveolins; hydrophobicity; protein transport; cell membrane

Abbreviations used in this paper: ADRP, adipocyte differentiation related protein; BFA, brefeldin A; DTAF, dichlorotriazinylaminofluorescein; FRT, Fischer rat thyroid; GAM, goat anti–mouse Ig(G + M); GAR, goat anti–rabbit IgG; GBV-B, GB virus-B; HCV, hepatitis C virus; IF, indirect immunofluorescence microscopy; LD, lipid droplet; PLAP, placental AP.

© The Rockefeller University Press, 0021-9525/2004/01/69/10 $8.00
The Journal of Cell Biology, Volume 164, Number 1, January 5, 2004 69–78
http://www.jcb.org/cgi/doi/10.1083/jcb.200303037

The Journal of Cell Biology

Downloaded from jcb.rupress.org on January 4, 2012

Published January 5, 2004

(Garcia et al., 2003; McManaman et al., 2003; Nakamura and Fujimoto, 2003; Targett-Adams et al., 2003). Rather, LD targeting of both perilipin A (Garcia et al., 2003) and ADRP (Targett-Adams et al., 2003) involves redundant, discontinuous sequences.

The second class of LD proteins, which includes oleosins and caleosins, are "integral" LD proteins. These proteins share a distinctive topology. Hydrophilic NH_2- and COOH-terminal cytoplasmic domains flank a central hydrophobic domain, which can range in length from ~30 to >70 residues (in the case of oleosins), and is presumed to be embedded in the hydrophobic LD core. The structure of the hydrophobic domain of oleosins is controversial. It may assume a β strand conformation, interacting with adjacent strands to form a parallel β sheet (Li et al., 1992, 2002), or may contain a central tight turn between two antiparallel β strands (Huang, 1992; Tzen et al., 1992), or may be α-helical (Lacey et al., 1998). HCV and GBV-B core proteins have also been included in the class of integral LD proteins (Hope et al., 2002). The central domains of these proteins are fairly hydrophobic, although they contain several charged residues.

Correct targeting of oleosins is known to depend on signal recognition particle and the Sec61 translocon (Beaudoin et al., 2000; Abell et al., 2002). Thus, integral LD proteins are probably cotranslationally inserted in the ER membrane and diffuse in the ER bilayer to access the surface of nascent LDs while these are still embedded in the ER membrane. Access to the LD surface is only possible because these proteins lack hydrophilic domains on the luminal side of the membrane, as such domains could not be accommodated in the hydrophobic LD core. As expected, no transmembrane LD proteins are known. Integral LD proteins are highly concentrated on the LD surface, presumably reflecting a high affinity for the LD surface relative to the ER.

The central hydrophobic domain is required for LD targeting of oleosins and HCV core (Hope and McLauchlan, 2000; Hope et al., 2002). In addition, a "Pro knot" motif, consisting of three closely-spaced Pro residues at the center of the long hydrophobic domain, is present in oleosins (Tzen et al., 1992) and is required for their LD targeting (Abell et al., 1997). A similar motif is present in caleosins (Naested et al., 2000). Two closely spaced Pro residues near the hydrophobic domains of HCV and GBV-B core proteins appear to play a similar role, as they are required for LD targeting of HCV core (Hope et al., 2002).

Caveolin proteins are components of cell-surface caveolae (Smart et al., 1999). Caveolins-1 and -2 are widely distributed among mammalian cell types and are normally coexpressed, whereas caveolin-3 is muscle specific. Caveolin-2 accumulates in the Golgi apparatus (Mora et al., 1999; Parolini et al., 1999) and in LDs (Fujimoto et al., 2001; Ostermeyer et al., 2001) unless caveolin-1, with which it heterooligomerizes, is coexpressed.

Caveolins can sometimes accumulate in LDs, where they may function in signaling and cholesterol balance (Fujimoto et al., 2001; Ostermeyer et al., 2001; Pol et al., 2001). Caveolins were found in LDs under the following four conditions: (1) when sequences in the NH_2-terminal hydrophilic domain were deleted, (2) when an ER-retrieval signal was linked to caveolin-1, (3) when caveolin-2 was expressed without caveolin-1, and (4) when cells were treated with brefeldin A (BFA) to block transport from the ER to the Golgi apparatus. We proposed the following model to unify these observations (Ostermeyer et al., 2001). Because caveolins have the same topology as the aforementioned integral LD proteins, we proposed that caveolins have a high affinity for LDs. We suggested that after synthesis, the proteins are usually rapidly packaged into transport vesicles, preventing them from reaching the surface of nascent LDs. The vesicle packaging mechanism can be saturated though, and certain caveolin mutants are not recognized. These conditions lead to accumulation of caveolins in the ER, and then to LD targeting via the same mechanism used by other integral LD proteins.

Caveolin-2 was initially proposed to have a higher affinity for LDs than the other caveolins (Fujimoto et al., 2001). However, caveolin-1 is also highly concentrated in LDs

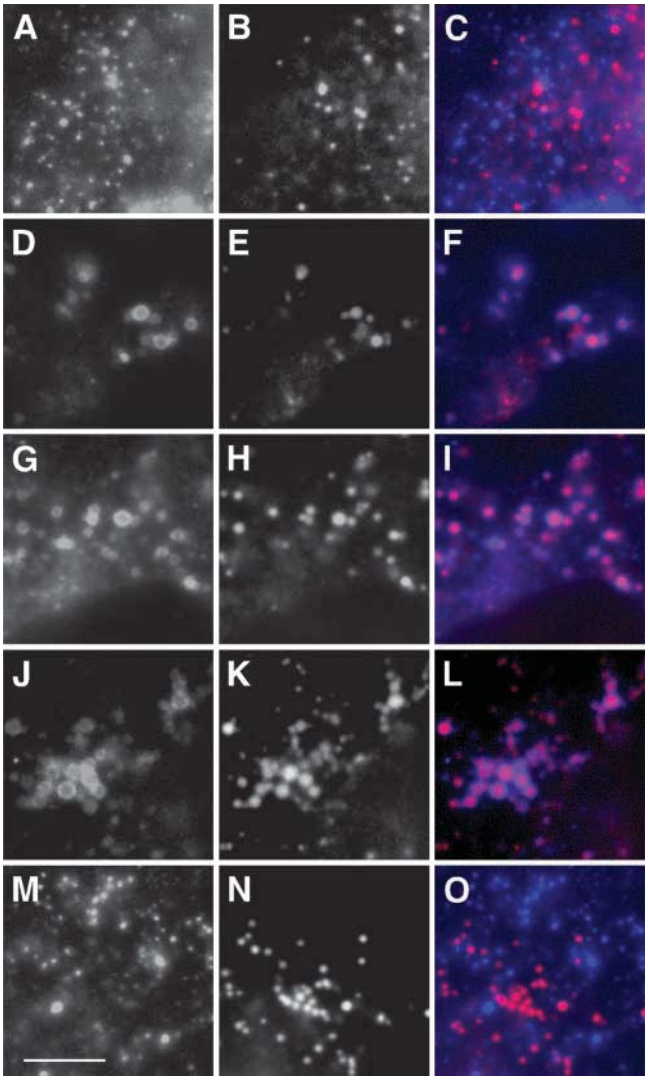

Figure 1. **Effect of drugs on LD accumulation of caveolin-1.** COS cells were left untreated (A–C) or treated with BFA alone (D–F) or BFA with nocodazole (G–I), cytochalasin B (J–L), or cycloheximide (M–O) for 5 h. Caveolin-1 was detected by IF with anti–caveolin-1 and Alexa Fluor 350-GAR (left) and LDs with Nile red (center). Right, merged images. Images were taken with a 100× objective. Each image shows a portion of one cell; for orientation, dark areas at lower right in F and I are the edges of nuclei. Bar, 5 μm.

Downloaded from jcb.rupress.org on January 4, 2012

Published January 5, 2004

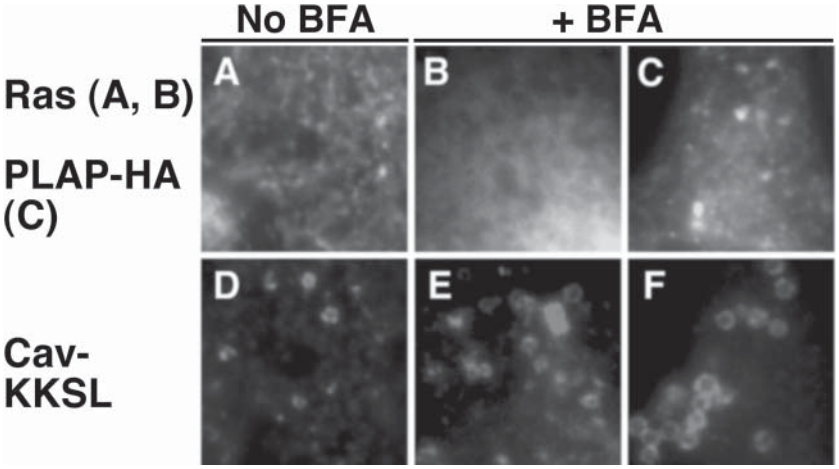

Figure 2. **Neither H-Ras nor the transmembrane protein PLAP-HA accumulate in LDs.** (A, B, D, and E) GFP-tagged nonpalmitoylated H-Ras (A and B) and Cav-KKSL (D and E) were coexpressed in COS cells. Cells were not treated (A and D; same cell) or treated (B and E; same cell) with BFA for 5 h. Mutant H-Ras was visualized by GFP fluorescence, and caveolin-KKSL by IF, using Texas red–GAR. (C and F) In one cotransfected, BFA-treated FRT cell, PLAP-HA was detected with anti-PLAP and FITC-GAR (C), and Cav-KKSL was detected with anti-myc and Texas red–GAM (F).

when linked to an ER retrieval signal (Ostermeyer et al., 2001). Caveolin-2 is transported inefficiently through the secretory pathway in the absence of caveolin-1 (Mora et al., 1999; Parolini et al., 1999). Thus, LD accumulation of caveolin-2 may result from inefficient transport out of the ER.

Here, we first provide further evidence that accumulation of caveolin-1 in the ER leads to LD targeting. To determine whether any protein on the cytosolic face of the ER that lacked transmembrane domains could concentrate in LDs, we examined H-Ras, which is initially targeted to the cytosolic face of the ER. Finally, a major goal of this work was to use caveolin-1 as model to define LD targeting signals.

Results

Caveolin-1 is normally concentrated in caveolae, and not in LDs, in COS cells (Fig. 1, A–C), but accumulates in LDs after 5 h of BFA treatment (Ostermeyer et al., 2001; Fig. 1, D–F). LDs were identified with the lipophilic dye Nile red (Fig. 1, B and E). Although not clear in Fig. 1, caveolin-1 also remained abundant in caveolae after BFA treatment. Here, we used the ability of BFA to induce LD accumulation of caveolin-1 to identify factors that blocked that targeting.

BFA-induced LD accumulation of caveolin-1 requires ongoing protein synthesis but not microtubules or microfilaments

To determine whether BFA-induced LD accumulation required an intact cytoskeleton, COS cells in which microtubules were disrupted with nocodazole, or microfilaments disrupted with cytochalasin B, were treated with BFA for 5 h. Neither drug inhibited BFA-induced LD accumulation (Fig. 1, G–L; although not depicted, LDs sometimes appeared clumped after nocodazole treatment). However, blocking protein synthesis with cycloheximide greatly reduced BFA-induced LD accumulation, and the protein was mostly seen in punctate caveolae (Fig. 1, M–O). Cycloheximide treatment did not affect LD density or size. These findings are consistent with our proposal that newly synthesized caveolin-1 enters nascent LDs by diffusion in the ER membrane and cannot enter LDs after leaving the ER (Ostermeyer et al., 2001).

Further experiments examining transfected proteins were performed either in COS or Fischer rat thyroid (FRT) cells, which lack endogenous caveolin-1 and caveolae, but can assemble exogenously expressed caveolin-1 into caveolae (Lipardi et al., 1998). The localization of caveolin-1 in transfected FRT cells is very similar to that in COS cells (Lipardi et al., 1998; Ostermeyer et al., 2001). In both cell types, we saw caveolin-1 in the Golgi apparatus as well as in caveolae, as reported previously (Dupree et al., 1993; Denker et al., 1996; Luetterforst et al., 1999).

H-Ras does not concentrate in LDs

To see if any overexpressed protein on the cytoplasmic surface of the ER entered LDs nonspecifically, we examined H-Ras, which is recruited to the ER after synthesis and reaches the plasma membrane via the secretory pathway (Choy et al., 1999). Ras proteins move slowly through the secretory pathway and are seen in the ER and Golgi apparatus at steady state. We saw no LD staining of EGFP–H-Ras expressed in COS cells (unpublished data). Because plasma membrane staining might have obscured LD staining, we expressed an EGFP mutant nonpalmitoylated H-Ras, which remains in the ER and Golgi apparatus and does not reach the cell surface (Choy et al., 1999). To identify LDs, we coexpressed Cav-KKSL (caveolin-1 with an appended ER retrieval motif), which accumulates in LDs even without BFA (Ostermeyer et al., 2001). Nonpalmitoylated H-Ras had a diffuse ER localization (Fig. 2, A and B) and was detected only rarely (<5% of transfected cells) in Cav-KKSL–positive LDs with or without BFA treatment.

A transmembrane protein is excluded from LDs after BFA treatment

To confirm that transmembrane proteins were excluded from LDs, we cotransfected FRT cells with Cav-KKSL and the hybrid protein placental AP (PLAP)–HA (Arreaza and Brown, 1995), treated them with BFA for 5 h, and processed them for indirect immunofluorescence microscopy (IF). As expected, PLAP-HA was never detected in LDs in FRT cells (Fig. 2 C) or in COS cells (not depicted).

BFA-induced LD targeting of caveolin mutants

In the rest of this work, we examined caveolin-1 mutants, attempting to identify sequences needed for LD targeting. We first examined mutants in BFA-treated FRT cells, searching for those that failed to accumulate in LDs. Mutants are sche-

Downloaded from jcb.rupress.org on January 4, 2012

Published January 5, 2004

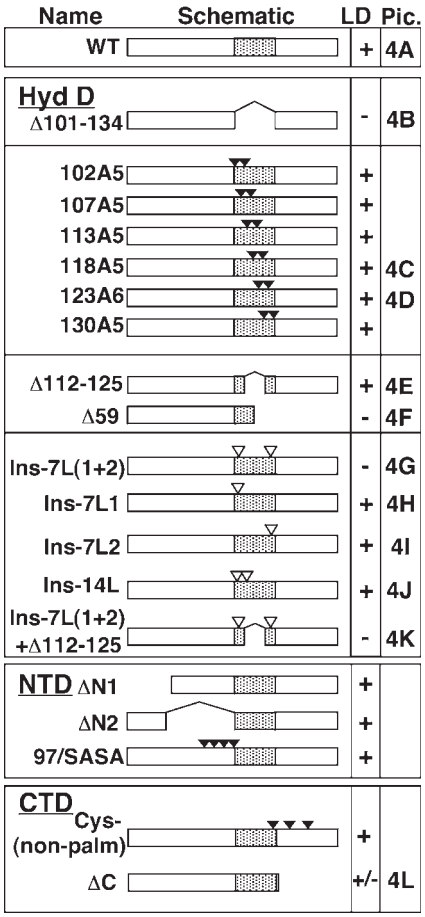

Figure 3. **BFA-induced LD accumulation of wild-type and mutant caveolin-1.** FRT cells expressing the indicated proteins were treated with BFA for 5 h, and caveolin-1 was detected by IF. Proteins are listed by name and diagrammed schematically (not to scale). The NH_2-terminal, hydrophobic, and COOH-terminal domains of caveolin-1 are schematized as open, shaded, and open boxes, respectively. Deletions are schematized as gaps, substitutions as closed triangles, and 7-Leu insertions as open triangles. Except for the hydrophobic domain mutants (102A5–130A5), the number of triangles corresponds to the number of changes. Mutants in the hydrophobic domain (Hyd D), NH_2-terminal domain (NTD), and COOH-terminal domain (CTD) are grouped together. Pic., IF images of these proteins are shown in the indicated panels of Fig. 4.

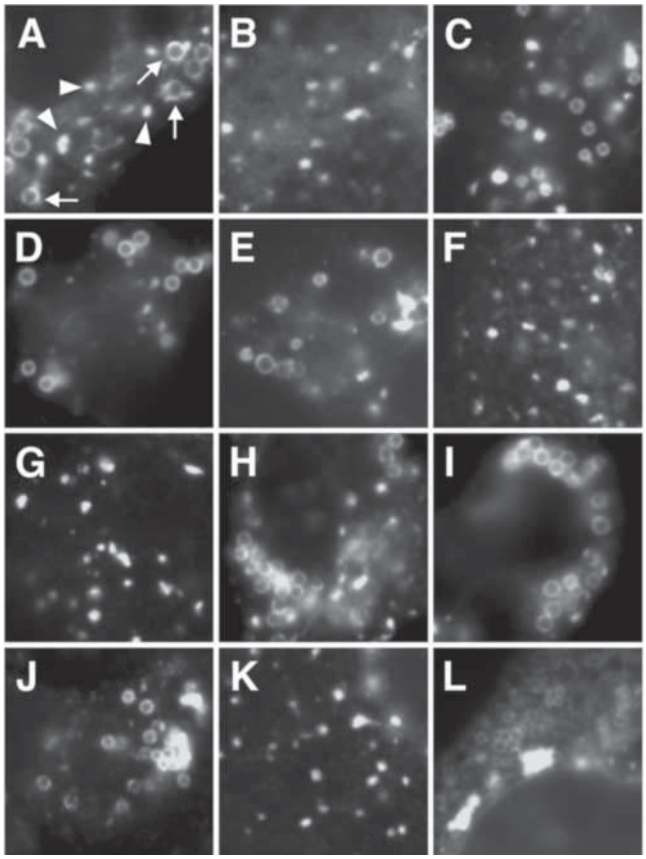

Figure 4. **Localization of wild-type and mutant caveolin-1 in BFA-treated FRT cells.** (A) Caveolin-1; (B) Δ101-134; (C) 118A5; (D) 123A6; (E) Δ112-125; (F) Δ59; (G) Ins7L(1+2); (H) Ins-7L1; (I) Ins-7L2; (J) Ins-14L; (K) Ins7L(1+2)+ Δ112-125; and (L) ΔC. Cells were treated with BFA for 5 h. Proteins were visualized by IF, using anticaveolin antibodies and DTAF-GAR. Arrows, LDs. Arrowheads, puncta staining for GM130 (not depicted), presumed to be ER exit sites.

matically diagrammed and the results are listed in Fig. 3, with pictures of selected mutants shown in Figs. 4 and 5. After BFA treatment, in FRT cells, as in COS cells, wild-type caveolin-1 was present in structures with the characteristic round shape of LDs (Fig. 4 A, arrows) that stained for the LD marker protein ADRP (Fig. 5, A–C) in 66 ± 15% ($n = 6$) of transfected cells after BFA treatment. Although the methanol fixation required for efficient detection of ADRP distorted LD shape, as reported previously (DiDonato and Brasaemle, 2003), colocalization of ADRP and caveolin was clear (Fig. 5, A–C). Caveolin-1 staining was also seen in caveolae, which did not stain for ADRP. Without BFA treatment, wild-type caveolin-1 was occasionally (~5% of cells) seen in LDs in FRT cells, in the very highest expressing cells (unpublished data). After BFA treatment, caveolin-1 and all the mutants examined were also seen in punctate structures larger than caveolae and distributed throughout the cell (Fig. 4 A, arrowheads). These structures did not stain for ADRP and were thus not related to LDs, but stained for GM130 (unpublished data), and are probably ER exit sites (Ward et al., 2001). The unusual behavior of caveolin-1 in concentrating in these structures in BFA-treated cells will be described elsewhere (unpublished data).

NH_2-terminal domain mutants

ΔN2, which lacks the downstream half of the NH_2-terminal domain (Δ46-95) of caveolin-1, accumulated in LDs with (Fig. 3) or without (Ostermeyer et al., 2001) BFA treatment. ΔN2 lacks a domain required for oligomerization of caveolin-1 (Sargiacomo et al., 1995) and migrated as a monomer on velocity gradients (unpublished data). Thus, oligomerization was not required for LD targeting of caveolin-1. A quadruple substitution mutant near the end of the NH_2-terminal domain, 97/SASA, showed efficient BFA-induced LD localization, as did ΔN1 (Δ3-48), which lacked most of the first half of the NH_2-terminal domain (Fig. 3). Because these mutants spanned the NH_2-terminal domain (except for S2, K96, and R101), no sequences in this domain were required for LD targeting. BFA-induced LD targeting of 97/SASA, chosen as a representative mutant, was verified by colocalization with ADRP (Fig. 5, D–F). BFA significantly reduced overall ADRP staining in FRT cells. However, expression of wild-type or mu-

Downloaded from jcb.rupress.org on January 4, 2012

Published January 5, 2004

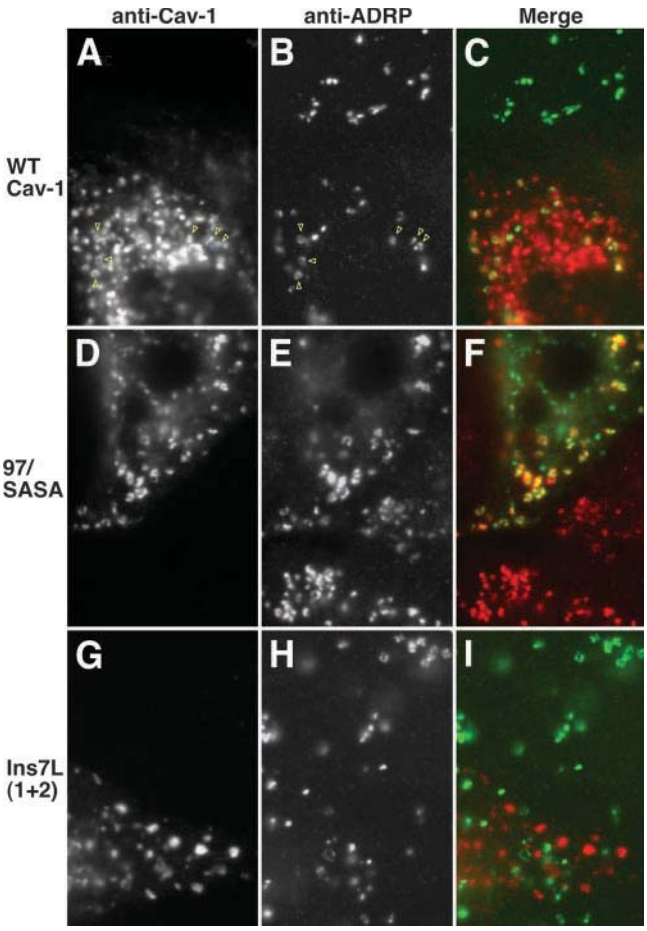

Figure 5. **Localization of wild-type and mutant caveolin-1 and ADRP in BFA-treated FRT cells.** FRT cells expressing caveolin-1 (A–C), 97/SASA (D–F), or Ins-7L(1+2) (G–I) were BFA treated for 4 h and methanol fixed. Caveolin and mutants were detected by IF, using (A and G) Texas red–GAR or (D) FITC-GAR. ADRP was detected in the transfected cells and neighboring untransfected cells using (B and H) DTAF-GAM or (E) Texas red–GAM. (C, F, and I) Merged images. (A and B) Yellow arrows indicate some regions of overlap.

tant caveolin-1 did not induce LD formation or alter LD density, as shown by comparison of ADRP staining in transfected and untransfected cells (Fig. 5; each panel shows two cells, only one of which was transfected). 97/SASA was not transported to the cell surface as efficiently as wild-type caveolin-1, explaining why this mutant was less prominent in ADRP-negative caveolae than was the wild-type protein (Fig. 5, compare C with F).

Hydrophobic domain mutants

As both the last 20 residues of the NH_2-terminal domain (Schlegel et al., 1999; Arbuzova et al., 2000) and the COOH-terminal domain (Luetterforst et al., 1999; Schlegel and Lisanti, 2000) of caveolin-1 can associate with membranes independently, the hydrophobic domain is not required for membrane association. A caveolin-1 mutant lacking the hydrophobic domain (Δ101-134) was detected in the Golgi apparatus and the plasma membrane by IF (unpublished data). However, this mutant was not seen in LDs after BFA treatment. Similar behavior was reported for an equivalent caveolin-2 mutant (Fujimoto et al., 2001). Instead, it was concentrated in punctate GM130-positive structures (Fig. 4 B). To determine the importance of specific hydrophobic domain residues in LD targeting, we examined a series of mutants in which sequential groups of five or six residues, through the hydrophobic domain, were changed to Ala. The mutants, named for the position of the first substitution and the number of substitutions, are diagrammed in Fig. 3, starting with 102A5. All of these mutants accumulated in LDs as efficiently as wild-type caveolin-1 after BFA treatment, as shown for 118A5 (Fig. 4 C) and 123A6 (Fig. 4 D). We conclude that no individual residues in the hydrophobic domain were required for LD targeting.

The next two caveolin-1 mutants suggested that the topology of the hydrophobic domain, rather than its length, might be important in LD targeting. We first deleted the central 14 residues from the hydrophobic domain, generating Δ112-125. Upon BFA treatment, this mutant was seen in LDs (Fig. 4 E). However, the mutant Δ59, which lacked the last 59 residues of the protein and ended in the middle of the hydrophobic domain (with no myc tag), did not concentrate in LDs after BFA treatment (Fig. 4 F). These differences were observed although the hydrophobic domains of Δ112-125 and Δ59 were very similar in length (18 residues in Δ59, 19 residues in Δ112-125).

Some insertion mutants are excluded from LDs

Next, we examined the effect of lengthening the hydrophobic domain of caveolin-1 on LD targeting. Although we do not know the conformation of the hydrophobic domain, we speculated that it might form two α helices, separated by a tight turn. This possibility guided us in making insertion mutants. With the aim of minimizing disruption of protein structure, we first inserted two groups of seven Leu (each group predicted to form two helix turns, if the structure were helical) into the hydrophobic domain, one near each end. The positions of the insertions were chosen to allow one helix turn of native sequence in the membrane before the insertion. The resulting protein, Ins-7L(1+2), was concentrated in the Golgi apparatus and could be detected on the plasma membrane in many untreated cells (unpublished data), suggesting that it was not grossly misfolded. However, Ins-7L(1+2) was not detected in LDs after BFA treatment (Fig. 4 G), but was instead concentrated in the ER (not depicted) and in GM130-positive puncta. Double labeling for caveolin-1 and ADRP confirmed LD exclusion of Ins-7L(1+2), and comparison of ADRP staining in transfected and untransfected cells showed that this mutant did not affect LD size or density (Fig. 5, G–I).

Next, we made several new mutants to determine why this double insertion mutant, Ins-7L(1+2), was excluded from LDs. Ins7L-1 and Ins7L-2 each contained only one of the two 7-Leu insertions present in Ins-7L(1+2). Both insertions accumulated in LDs after BFA treatment (Fig. 4, H and I). For unknown reasons, Ins-7L-2 accumulated in LDs as well as the Golgi apparatus, even without BFA treatment.

Thus, exclusion of the double insertion mutant Ins-7L(1+2) from LDs did not result from disruption of an LD targeting signal by either insertion. Instead, it was possible that simply increasing the length of the hydrophobic span by 14 residues prevented LD targeting. To test this idea, we made two new double insertion mutants. A second group of 7 Leu was inserted in the hydrophobic domain of Ins-7L-1

Downloaded from jcb.rupress.org on January 4, 2012

Published January 5, 2004

close to the site of the first insertion, generating Ins-14L, which thus contained 14 Leu inserted near the NH_2-terminal end of the hydrophobic domain. BFA-induced LD accumulation of Ins-14L was similar to wild type (Fig. 4 J), suggesting that exclusion of Ins-7L(1+2) (the original double insertion mutant) from LDs did not result simply from the increased length of its hydrophobic domain. Another mutant, (Ins-7L(1+2)/Δ112-125), supported this conclusion. To make the mutant, we deleted the central 14 residues from the hydrophobic domain of Ins-7L(1+2). Thus, this mutant contained both of the original 7-Leu insertions, but its hydrophobic span was the same length as that of wild-type caveolin-1. Like Ins-7L(1+2), this mutant was virtually never detected in LDs after BFA treatment (Fig. 4 K). This finding suggested that the failure of Ins-7L(1+2) to target to LDs did not result from its increased hydrophobic span length.

To explain these results, we speculated that the bulky Leu side chains on the inserted residues in Ins-7L(1+2) blocked LD targeting through a steric effect by preventing proper packing of the residues in the hydrophobic domain with each other or with other proteins in the bilayer. According to this model, such an effect of either insertion alone could be tolerated, but both together would be prohibitive.

Expression level of hydrophobic domain mutants does not correlate with LD localization

To ensure that apparent exclusion of certain mutants from LDs did not result from low expression, we compared the expression levels of selected mutants (Fig. 6). Mutants were coexpressed with PLAP-HA as a transfection and loading control. Expression levels of different mutants varied widely. Although expression of Ins-7L(1+2) was quite low, two other mutants that failed to accumulate in LDs, Δ59 and Ins-7L(1+2)+Δ112-125, were expressed well (Fig. 6, lanes 1–6). Thus, expression levels of the hydrophobic domain mutants did not correlate with LD accumulation.

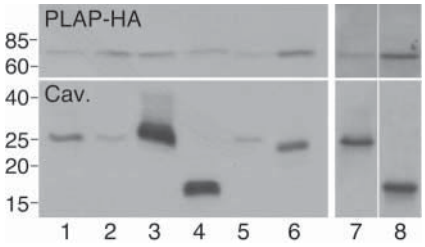

Figure 6. **Expression level of caveolin-1 mutants does not correlate with LD targeting.** FRT cells were cotransfected with PLAP-HA (as a transfection and loading control) and either Ins-7L1 (lane 1), Ins-7L2 (lane 2), Ins-7L(1+2)+Δ112-125 (lane 3), Δ59 (lane 4), Ins-7L(1+2) (lane 5), or Δ112-125 (lane 6); or, in a separate experiment, analyzed on a separate gel with Ins-7L(1+2) (lane 7) or ΔC (lane 8). Cells were lysed with gel loading buffer and proteins in equal aliquots of lysate were analyzed by SDS-PAGE and Western blotting. Blots were cut, and the tops were probed with anti-PLAP antibodies and the bottoms with anticaveolin antibodies. Both halves were probed with HRP–donkey anti–rabbit IgG, and proteins were visualized by ECL.

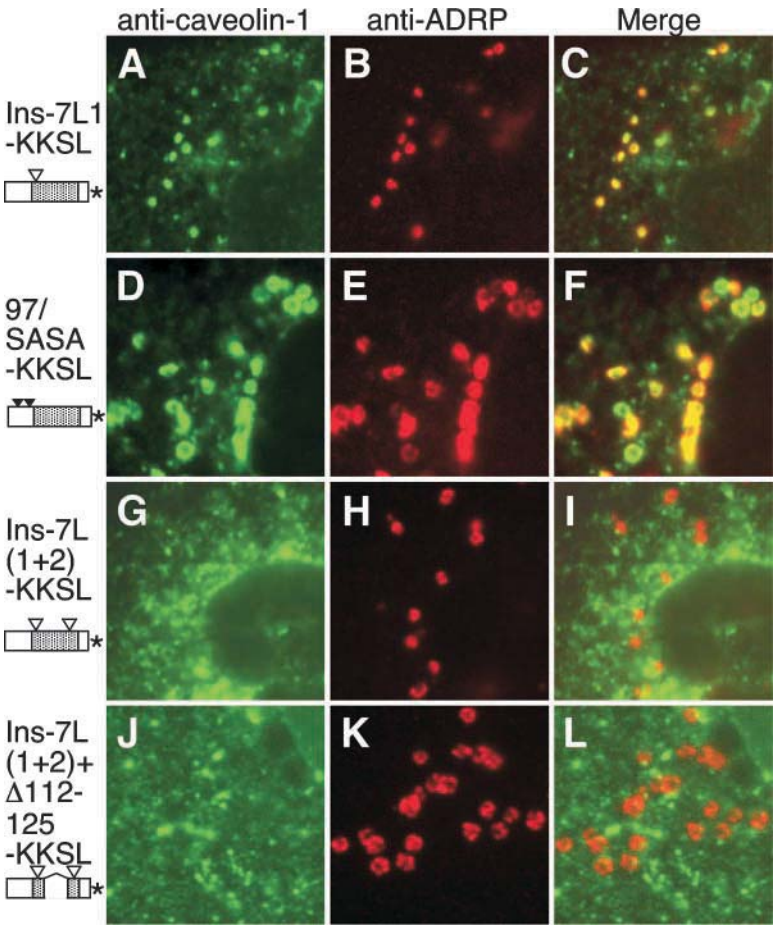

Figure 7. **Localization of KKSL-tagged caveolin-1 mutants.** FRT cells expressing Ins-7L1-KKSL (A–C), 97/SASA-KKSL (D–F), Ins-7L(1+2)-KKSL (G–I), or Ins-7L(1+2)+Δ112-125-KKSL (J–L) were methanol fixed. Caveolin-1 proteins (A, D, G, and J) and ADRP in the same cells (B, E, H, and K) were detected by IF. (C, F, I, and L) Merged images. Schematic depictions of proteins are as in Fig. 3, except that only two triangles indicate the four substitutions in 97/SASA. *, KKSL tag.

Downloaded from jcb.rupress.org on January 4, 2012

Published January 5, 2004

The COOH-terminal domain may contribute to LD targeting

Cys−, a nonpalmitoylated triple Cys-Ser caveolin-1 mutant (Dietzen et al., 1995), accumulated in LDs as well as the wild-type protein (Fig. 3), showing that palmitoylation was not required for LD targeting. A mutant lacking the entire COOH-terminal domain, ΔC, was localized to the plasma membrane and Golgi apparatus in untreated cells (unpublished data), unlike a similar caveolin-2 mutant, which was concentrated in the ER (Fujimoto et al., 2001). In BFA-treated cells, ΔC was detected in LDs in fewer cells (30 ± 7% of transfected cells, $n = 5$) than wild-type caveolin-1, and LD staining, relative to staining of GM130-positive puncta, was dimmer. Staining of the ER, including the nuclear envelope, was more prominent, suggesting a reduced affinity for LDs (Fig. 4 L). However, ΔC was expressed very poorly, at a level similar to or less than Ins-7L(1+2) (Fig. 6, lanes 7 and 8). Thus, the apparent partial reduction in LD targeting efficiency may have resulted from decreased expression.

LD targeting of KKSL-tagged mutants

To ensure that our results did not depend on BFA treatment, we appended KKSL ER retrieval tags to selected caveolin-1 mutants. Wild-type Cav-KKSL accumulates in LDs even without BFA (Ostermeyer et al., 2001). Similarly, KKSL-tagged forms of 97/SASA and Ins-7L1 were detected in LDs in virtually every expressing cell (Fig. 7). This contrasted with the localization of the non-KKSL tagged versions of the same proteins in BFA-treated cells, in which LD localization was detected in 60–80% of the cells. Increased LD accumulation of the KKSL-tagged proteins probably resulted from the fact that they were continuously retrieved to the ER, instead of accumulating there for only 5 h during BFA treatment. Nevertheless, KKSL-tagged forms of Ins-7L(1+2) and Ins-7L(1+2)+Δ112-125 were never seen in LDs (Fig. 7), although Ins-7L(1+2)-KKSL was expressed about as well as wild-type Cav-KKSL, 97/SASA-KKSL, and Ins-7L1-KKSL. Ins-7L(1+2)+Δ112-125-KKSL was expressed at a higher level (unpublished data). Thus, the inability of certain mutants to accumulate in LDs did not depend on BFA treatment.

Caveolin-1 mutants in isolated LDs

To confirm the IF results, we examined LDs isolated from transfected FRT cells for the presence of wild-type Cav-KKSL or selected KKSL-tagged mutants (Fig. 8). Aliquots of whole cell homogenate (Fig. 8, WC) and isolated LDs (Fig. 8, LD) from transfected FRT cells were probed for calnexin (to monitor ER contamination of the LD fraction), ADRP (to monitor LD yield), and various caveolin mutants (to monitor expression and LD targeting). In agreement with the IF results, wild-type Cav-KKSL and 97/SASA-KKSL were present in LDs, whereas Ins-7L(1+2)-KKSL and Ins-7L(1+2)+Δ112-125-KKSL were largely excluded from LDs (Fig. 8).

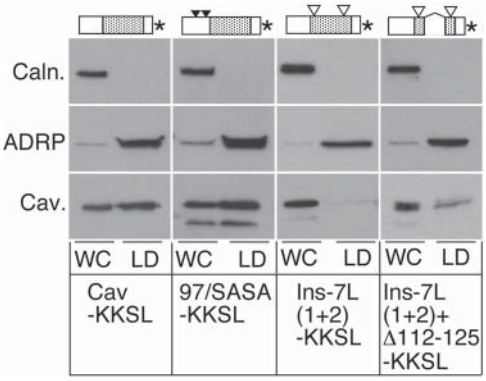

Figure 8. **KKSL-tagged caveolin-1 mutants in isolated LDs.** LDs were isolated from oleic acid–treated FRT cells expressing Cav-KKSL, 97/SASA-KKSL, Ins-7L(1+2)-KKSL, or Ins-7L(1+2)+Δ112-125-KKSL as indicated. Proteins in the LDs (LD) or in a reserved 5% of the whole cell homogenate (WC) were analyzed by SDS-PAGE and Western blotting and detected by ECL. Blots were cut in three parts. Top, probed with anticalnexin and HRP-donkey anti–rabbit IgG. Middle, anti-ADRP and HRP-GAM. Bottom, anticaveolin and HRP-donkey anti–rabbit IgG. Schematic depictions of proteins are as in Fig. 7.

Discussion

We provided additional support for our model of LD targeting of caveolin-1 (Ostermeyer et al., 2001). In this model, we suggested that when caveolins accumulate in the ER, they reach the surface of nascent LDs by diffusion in the ER membrane. Consistent with this idea, BFA-induced LD targeting of caveolin-1 did not require microtubules or microfilaments. The model predicts that caveolin-1 must be in the ER at the time of BFA treatment to enter LDs. As predicted, treatment of cells with cycloheximide to prevent new caveolin-1 synthesis and ER insertion during BFA treatment prevented BFA-induced LD accumulation.

Although this model explains how caveolins reach the LD surface, it does not explain why they become so concentrated there. Nonpalmitoylated H-Ras, whose ER localization and topology suggest it should be able to reach LDs as well as caveolins, never accumulated there. Thus, our second goal was to learn why caveolins have such a high affinity for LDs.

Importance of the hydrophobic domain in LD targeting

The hydrophobic domain, though no specific sequences therein, was required for LD targeting of caveolin-1. In contrast, the hydrophobic domain was not essential for membrane association of caveolin-1. Thus, membrane association was not sufficient for LD targeting. Several pieces of evidence suggested that the unusual topology of caveolin-1, with two cytoplasmic domains flanking a central hydrophobic domain, is a crucial determinant of LD targeting of integral proteins. First, bona fide integral LD proteins, oleosins and caleosins, have the same topology (Huang, 1992; Chen et al., 1999). Second, caveolin-1 mutants that lacked the entire hydrophobic domain or that ended after the first half of the domain were not targeted to LDs. Similarly, a caveolin-2 mutant that lacked the hydrophobic domain was not detected in LDs (Fujimoto et al., 2001). Nevertheless, mutational analysis showed that no specific residues in the hydrophobic domain were essential for LD targeting. This finding showed that a Pro knot motif, shown to be important in LD targeting of oleosins (Abell et al., 1997) and HCV core (Hope et al., 2002), is not universally required for LD targeting of integral proteins.

Downloaded from jcb.rupress.org on January 4, 2012

Published January 5, 2004

Leu insertions in the hydrophobic domain can block LD targeting of caveolin-1

Although no residues in the hydrophobic domain of caveolin-1 were absolutely required, certain insertion mutations in this domain greatly reduced LD targeting. Inserting two 7-Leu segments into the hydrophobic domain, one near each end, blocked LD targeting. LD targeting was blocked even when the central 14 residues of the hydrophobic domain were also deleted to restore the normal length of the hydrophobic domain. Simply deleting the 14 central hydrophobic residues from the wild-type protein, to shorten the domain, did not block LD targeting. LD targeting of mutants containing only one 7-Leu insertion was not affected. Similarly, inserting two 7-Leu segments, both near the NH_2-terminal end of the hydrophobic domain, did not block LD targeting. Thus, the position of the inserted Leu residues in the hydrophobic domain, rather than their number or total hydrophobic domain length, could affect LD targeting.

Leu insertions might affect hydrophobic helix packing

The fact that we do not know the structure of the hydrophobic domain of caveolin-1 limits interpretation of our results. However, an attractive model is that this domain forms two α helices, which are separated by a tight turn. The need to satisfy backbone hydrogen bonds places severe constraints on the possible conformations of lipid-embedded protein domains. With the exception of β barrel structures in certain bacterial proteins, all known transmembrane peptides are α-helical (Monné et al., 1999). It is important to note, though, that the hydrophobic domain of oleosins has been suggested to form an extended β strand that aligns parallel to strands in adjacent molecules (Li et al., 2002), although others have suggested that the domain is helical (Lacey et al., 1998). Nevertheless, a model protein with a hydrophobic domain as short as 31 residues was shown to be able to form a helix-turn-helix motif, without an absolute requirement for Pro at the turn (Monné et al., 1999). Thus, we will next consider a model for how Leu insertions might affect LD targeting of caveolin-1 if the hydrophobic domain were to form a helix-turn-helix motif.

As schematized in Fig. 9 (A and B), we suggest that proper packing of the two putative hydrophobic helices is important in LD targeting of caveolin-1. Seven Leu would form two turns of an α helix. We speculate that the bulky Leu side chains interfere with correct packing of the helices with each other, or with other membrane proteins. One 7-Leu insertion alone or insertion of 14 Leu near one end of the hydrophobic domain might be tolerated. However, simultaneous insertion of seven Leu into both helices might disrupt helix packing enough to block LD targeting, particularly if the helices normally pack against each other. Consistent with this possibility, as shown in Fig. 9 C, one face of a helix formed by the first half of the hydrophobic domain would consist entirely of Gly and Ala, whose small side chains are highly favored on hydrophobic helix faces that pack closely with other helices in membranes (Eilers et al., 2002).

The COOH-terminal domain of caveolin-1 may enhance LD targeting, although the reduced expression of ΔC limits the certainty of this conclusion. However, it is notable that the hydrophobic domain of caveolin-2 alone, fused to EGFP, did not localize to LDs (Fujimoto et al., 2001). This

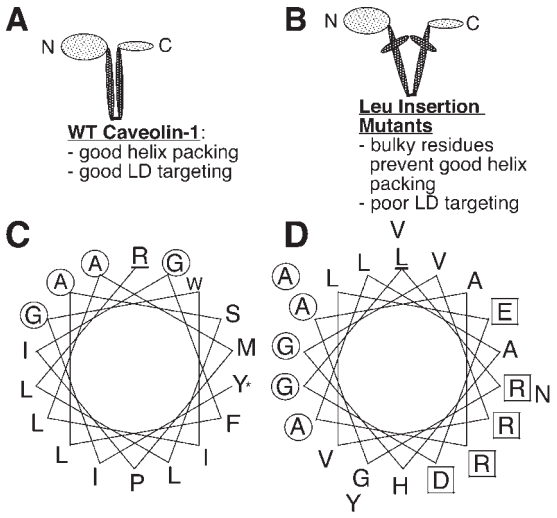

Figure 9. **Model depicting role of hydrophobic helix packing in LD targeting of caveolin-1.** We speculate here that the hydrophobic domain of caveolin-1 forms two α helices separated by a tight turn. (A) We propose that correct packing of the putative hydrophobic helices is required for LD targeting of wild-type caveolin-1. (B) Insertion of bulky Leu residues in both helices could inhibit LD targeting sterically by preventing proper helix packing. (C) Helical wheel depiction of the first half of the hydrophobic domain of caveolin-1 (R101 at the membrane interface [underlined] through Y119 [*]). Circles, residues on a Gly + Ala–rich helix face. (D) L144 (underlined) through A165 of the core coding region of HCV strain Glasgow (genotype 1a; Hope and McLauchlan, 2000), just downstream of the P138 + P143 motif, modeled as an α helix. Circles, residues on a Gly + Ala–rich helix face. Squares, charged residues.

is consistent with the idea that other sequences in caveolin-1, in addition to the hydrophobic domain, are required for LD targeting. Such sequences (possibly including the COOH-terminal domain) may facilitate LD targeting by stabilizing correct packing of the hydrophobic domain.

Role of the Pro knot in LD targeting

The precise role of the Pro knot motif in LD targeting of oleosins (and probably caleosins) and HCV core (Hope et al., 2002) is not known. In oleosins, this motif lies in the center of the 70-residue hydrophobic domain, where it has been proposed to induce formation of a 180° turn (Tzen et al., 1992). It might be imagined that the two resulting 35-residue hydrophobic helices (or, possibly, β-sheet structures; Huang, 1992) are too long to fit well in the ER bilayer. Thus, one model is that the Pro knot forces formation of helices that are too long for the bilayer but can be accommodated in LDs.

This model is less appealing in explaining the role of the Pro knot in LD targeting of other proteins. First, their hydrophobic domains are much shorter than those of oleosins and could easily be accommodated in bilayers, which can accommodate helical hairpins (Monné et al., 1999). Furthermore, although the central domains of HCV and GBV-B core proteins are more hydrophobic than adjacent domains, they contain several charged residues and could form amphipathic helices, as illustrated for the 24 residues downstream of the Pro knot of HCV core (Fig. 9 D). One face of this putative helix contains almost exclusively charged residues (Fig. 9 D, squares), and is unlikely to be completely embedded in a bilayer or an LD. Instead, a helix formed

Downloaded from jcb.rupress.org on January 4, 2012

Published January 5, 2004

by these residues would probably lie parallel to the surface, like other amphipathic helices (Johnson and Cornell, 1999). Similarly, the Pro knot in caleosins is at the end of the hydrophobic domain, adjacent to a highly charged sequence that could form an amphipathic helix (Naested et al., 2000). Thus, the Pro motif probably does not generally act in LD targeting by forcing formation of excessively long hydrophobic helices.

Is proper hydrophobic domain packing generally required for LD targeting?

We have suggested that proper hydrophobic helix packing may be important in LD targeting of caveolins. This may be true of other LD proteins as well. Lipid-embedded helices generally pack more tightly than helices in soluble proteins (Eilers et al., 2000), and we speculate that tight packing might be especially important in LD proteins. A helix formed by the 24 residues downstream of the Pro knot in HCV core would have a Gly + Ala–rich face (Fig. 9 D, circles). Also, the NH_2-terminal half of the hydrophobic domain of oleosins is unusually rich in Gly, Ala, and Ser (Tzen et al., 1992), which are favored at contact sites between membrane-embedded helices (Eilers et al., 2002). The Pro knot may act in LD targeting by affecting hydrophobic helix packing. Caveolins may achieve the same end (correct packing) by a different mechanism. It is even possible that the puzzling results of studies on LD targeting of ADRP and perilipins (Garcia et al., 2003; Targett-Adams et al., 2003) reflect a requirement for apparently redundant LD targeting motifs to pack together correctly for optimal LD targeting.

Despite the fact that LDs are present in most eukaryotic cells, surprisingly little is known about their synthesis or metabolism, or about how proteins are targeted to their surface. Our findings suggest that correct hydrophobic domain packing may be crucial for LD targeting of caveolins and possibly of other proteins as well. Further work will be required to learn how this targeting works and how LD proteins function.

Materials and methods

Cells and reagents

FRT and COS-1 cells have been described previously (Ostermeyer et al., 2001). Primary antibodies used were as follows: rabbit anti–caveolin-1 and mouse anti-GM130 (Transduction Laboratories); mouse antiadipophilin/ADRP (Research Diagnostics); rabbit anti-PLAP (DakoCytomation); mouse anti-myc (Invitrogen); rabbit anticalnexin (Manganas et al., 2001; gift of J. Trimmer, University of California, Davis, Davis, CA). Secondary antibodies used were as follows: dichlorotriazinylaminofluorescein (DTAF)-goat anti–mouse Ig(G + M) (GAM), FITC-goat anti–rabbit IgG (GAR), Texas red–GAR and GAM, HRP-GAM and HRP-donkey anti–rabbit IgG (Jackson ImmunoResearch Laboratories), and Alexa Fluor 350-GAR (Molecular Probes). Lipofectamine 2000 was obtained from GIBCO BRL, and other reagents were obtained from Sigma-Aldrich.

Plasmids

Plasmids encoding GFP–H-Ras and the nonpalmitoylated GFP–H-RasC181S,C184S (Choy et al., 1999) were gifts of M. Philips (New York University, New York, NY). A plasmid encoding the hybrid protein PLAP-HA, containing the extracellular domain of PLAP and the transmembrane and cytoplasmic domains of influenza hemagglutinin, has been described previously (Arreaza and Brown, 1995). Plasmids encoding NH_2-terminal HA-tagged and COOH-terminal myc-tagged canine caveolin-1 (α isoform), a nonpalmitoylated mutant of this protein (Cys−), and Cav-ΔN2 (referred to here as ΔN2) have been described previously (Dietzen et al., 1995; Ostermeyer et al., 2001). Additional canine caveolin-1 mutants were generated using the QuikChange site-directed mutagenesis kit (Stratagene) or by PCR and verified by sequencing. Non–self-explanatory mutants are as follows, using the residue numbers in canine caveolin-1 α: Ins-7L(1 + 2), insertion of seven Leu after A105 and seven Leu after V130; Ins-7L1, insertion of seven Leu after A105; Ins-7L2, insertion of seven Leu after V130; Ins-14L, insertion of seven Leu after A105, and seven Leu after I109. The names 102A5, 107A5, 113A5, 118A5, 123A6, and 130A5 refer to substitution of Ala for the indicated number of residues (5–6), starting with the indicated residue. 97/SASA; Y97, W98, F99, Y100 changed to SASA, respectively. ΔN1, lacks G3-E48; ΔN2, lacks T46-T95; ΔC, lacks S136-T178; and Δ59, lacks A120-T178. All mutants contained an NH_2-terminal HA tag. All except Δ59 contained a COOH-terminal myc tag.

Procedures

Cells were transiently transfected using Lipofectamine 2000 and observed 1 or 2 d after transfection. IF using an epifluorescence microscope (model Axioskop 2; Carl Zeiss MicroImaging, Inc.) was as described previously (Ostermeyer et al., 2001), except that PFA fixation and permeabilization were performed at 25–27°C, and methanol fixation (10 min, 0°C) was used for detection of the LD marker protein ADRP (Brasaemle et al., 1997b). Although this distorted LD shape (DiDonato and Brasaemle, 2003), colocalization of ADRP and caveolin on LDs could be detected. All images were obtained with a 100× objective (NA = 1.3). Images were captured with a SPOT cooled CCD 24-bit color digital camera (Diagnostic Instruments, Inc.) and processed using Adobe Photoshop. Where indicated, cells were incubated with media containing 10 μg/ml BFA, 50 μg/ml cycloheximide, 10 μg/ml cytochalasin B, and/or 10 μM nocodazole for 5 h before fixation.

In IF experiments, wild-type and mutant caveolin-1 were detected with anti–caveolin-1 antibodies and DTAF-GAR, except as noted next. When coexpressed with PLAP-HA, caveolin-1 was detected with anti-myc antibodies. For colocalization with Nile red, caveolin-1 was detected with blue Alexa Fluor 350 GAR secondary antibodies, though resolution was lower than with DTAF-GAR, because the fluorescence absorbance profile of Nile red overlaps with both DTAF (green) and with Texas red.

LD isolation from oleic acid–treated FRT cells and recovery of LD proteins by acetone precipitation were performed as described previously (Garcia et al., 2003) with the following minor modifications. Oleic acid–defatted BSA complexes were added to cells in one confluent 10-cm dish 5 h after transfection. The next day, cells were scraped from the dish, washed in PBS, washed in homogenization buffer (10 mM Hepes, pH 7.4, and 5 mM EDTA), resuspended in 200 μl homogenization buffer with protease inhibitors (1 μg/ml pepstatin, 0.2 mM PMSF, and 1 μg/ml leupeptin), and homogenized by 35 passages through a 25-gauge needle. An aliquot of homogenate was reserved. The remainder was adjusted to 1 ml with homogenization buffer with protease inhibitors and subjected to centrifugation at 100,000 *g* for 30 min in an ultracentrifuge (model Optima TL; Beckman Coulter). The top 200 μl, containing the LDs, was harvested, and LD proteins were collected by acetone precipitation. SDS-PAGE, transfer to nylon membranes, and Western blotting were performed as described previously (Schroeder et al., 1998).

We thank M. Philips for plasmids, J. Trimmer for anticalnexin antibodies, and N. Dean and members of the Brown laboratory for reading the manuscript.

This work was supported by grants GM47897 (to D.A. Brown) and GM41297 (to D.M. Lublin) from the National Institutes of Health.

Submitted: 6 March 2003
Accepted: 25 November 2003

References

Abell, B.M., I.A. Holbrook, M. Abenes, D.J. Murphy, M.J. Hills, and M.M. Moloney. 1997. Role of the proline knot motif in oleosin endoplasmic reticulum topology and oil body targeting. *Plant Cell.* 9:1481–1493.

Abell, B.M., S. High, and M.M. Moloney. 2002. Membrane topology of oleosin is constrained by its long hydrophobic domain. *J. Biol. Chem.* 277:8602–8610.

Arbuzova, A., L. Wang, J. Wang, G. Hangyas-Mihalyne, D. Murray, B. Honig, and S. McLaughlin. 2000. Membrane binding of peptides containing both basic and aromatic residues. Experimental studies with peptides corresponding to the scaffolding region of caveolin and the effector region of MARCKS. *Biochemistry.* 39:10330–10339.

Arreaza, G., and D.A. Brown. 1995. Sorting and intracellular trafficking of a glycosylphosphatidylinositol-anchored protein and two hybrid proteins with the same ectodomain in MDCK kidney epithelial cells. *J. Biol. Chem.* 270: 23641–23647.

Barba, G., F. Harper, T. Harada, M. Kohara, S. Goulinet, Y. Matsuura, G. Eder, Z. Schaf, M.J. Chapman, T. Miyamura, and C. Brechot. 1997. Hepatitis C virus core protein shows a cytoplasmic localization and associates to cellular lipid storage droplets. *Proc. Natl. Acad. Sci. USA.* 94:1200–1205.

Downloaded from jcb.rupress.org on January 4, 2012

Published January 5, 2004

Beaudoin, F., B.M. Wilkinson, C.J. Stirling, and J.A. Napier. 2000. In vivo targeting of a sunflower oil body protein in yeast secretory (sec) mutants. *Plant J.* 23:159–170.

Brasaemle, D.L., T. Barber, A.R. Kimmel, and C. Londos. 1997a. Post-translational regulation of perilipin expression. Stabilization by stored intracellular neutral lipids. *J. Biol. Chem.* 272:9378–9387.

Brasaemle, D.L., T. Barber, N.E. Wolins, G. Serrero, E.J. Blanchette-Mackie, and C. Londos. 1997b. Adipose differentiation-related protein is an ubiquitously expressed lipid storage droplet-associated protein. *J. Lipid Res.* 38:2249–2263.

Chen, J.C., C.C. Tsai, and J.T. Tzen. 1999. Cloning and secondary structure analysis of caleosin, a unique calcium- binding protein in oil bodies of plant seeds. *Plant Cell Physiol.* 40:1079–1086.

Choy, E., V.K. Chiu, J. Silletti, M. Feoktistov, T. Morimoto, D. Michaelson, I.E. Ivanov, and M.R. Philips. 1999. Endomembrane trafficking of ras: the CAAX motif targets proteins to the ER and Golgi. *Cell.* 98:69–80.

Denker, S.P., J.M. McCaffrey, G.E. Palade, P.A. Insel, and M.G. Farquhar. 1996. Differential distribution of α subunits and βγ subunits of heterotrimeric G proteins on Golgi membranes of the exocrine pancreas. *J. Cell Biol.* 133:1027–1040.

DiDonato, D., and D.L. Brasaemle. 2003. Fixation methods for the study of lipid droplets by immunofluorescence microscopy. *J. Histochem. Cytochem.* 51: 773–780.

Dietzen, D.J., W.R. Hastings, and D.M. Lublin. 1995. Caveolin is palmitoylated on multiple cysteine residues: palmitoylation is not necessary for localization of caveolin to caveolae. *J. Biol. Chem.* 270:6838–6842.

Dupree, P., R.G. Parton, G. Raposo, T.V. Kurzchalia, and K. Simons. 1993. Caveolae and sorting in the trans-Golgi network of epithelial cells. *EMBO J.* 12: 1597–1605.

Egan, J.J., A.S. Greenberg, M. Chang, S.A. Wek, M.C.J. Moos, and C. Londos. 1992. Mechanism of hormone-stimulated lipolysis in adipocytes: translocation of hormone-sensitive lipase to the lipid storage droplet. *Proc. Natl. Acad. Sci. USA.* 89:8537–8541.

Eilers, M., S.C. Shekar, T. Shieh, S.O. Smith, and P.J. Fleming. 2000. Internal packing of helical membrane proteins. *Proc. Natl. Acad. Sci. USA.* 97:5796–5801.

Eilers, M., A.B. Patel, W. Liu, and S.O. Smith. 2002. Comparison of helix interactions in membrane and soluble alpha-bundle proteins. *Biophys. J.* 82: 2720–2736.

Fujimoto, T., H. Kogo, K. Ishiguro, K. Tauchi, and R. Nomura. 2001. Caveolin-2 is targeted to lipid droplets, a new "membrane domain" in the cell. *J. Cell Biol.* 152:1079–1086.

Garcia, A., A. Sekowski, V. Subramanian, and D.L. Brasaemle. 2003. The central domain is required to target and anchor perilipin A to lipid droplets. *J. Biol. Chem.* 278:625–635.

Hope, R.G., and J. McLauchlan. 2000. Sequence motifs required for lipid droplet association and protein stability are unique to the hepatitis C virus core protein. *J. Gen. Virol.* 81:1913–1925.

Hope, R.G., D.J. Murphy, and J. McLauchlan. 2002. The domains required to direct core proteins of hepatitis C virus and GB virus-B to lipid droplets share common features with plant oleosin proteins. *J. Biol. Chem.* 277:4261–4270.

Huang, A.H.C. 1992. Oil bodies and oleosins in seeds. *Annu. Rev. Plant Physiol. Plant Mol. Biol.* 43:177–200.

Johnson, J.E., and R.B. Cornell. 1999. Amphitropic proteins: regulation by reversible membrane interactions (review). *Mol. Membr. Biol.* 16:217–235.

Lacey, D.J., N. Wellner, F. Beaudoin, J.A. Napier, and P.R. Shewry. 1998. Secondary structure of oleosins in oil bodies isolated from seeds of safflower (*Carthamus tinctorius L.*) and sunflower *(Helianthus annuus L.). Biochem. J.* 334:469–477.

Li, M., L.J. Smith, D.C. Clarke, R. Wilson, and D.J. Murphy. 1992. Secondary structures of a new class of lipid body proteins from oilseeds. *J. Biol. Chem.* 267:8245–8253.

Li, M., D.J. Murphy, K.-H.K. Lee, R. Wilson, L.J. Smith, D.C. Clark, and J.-Y. Sung. 2002. Purification and structural characterization of the central hydrophobic domain of oleosin. *J. Biol. Chem.* 277:37888–37895.

Lipardi, C., R. Mora, V. Colomer, S. Paladino, L. Nitsch, E. Rodriguez-Boulan, and C. Zurzolo. 1998. Caveolin transfection results in caveolae formation but not apical sorting of glycosylphosphatidylinositol (GPI)-anchored proteins in epithelial cells. *J. Cell Biol.* 140:617–626.

Londos, C., D.L. Brasaemle, C.J. Schultz, J.P. Segrest, and A.R. Kimmel. 1999. Perilipins, ADRP, and other proteins that associate with intracellular neutral lipid droplets in animal cells. *Semin. Cell Dev. Biol.* 10:51–58.

Luetterforst, R., E. Stang, N. Zorzi, A. Carozzi, M. Way, and R.G. Parton. 1999. Molecular characterization of caveolin association with the Golgi complex: identification of a cis-Golgi targeting domain in the caveolin molecule. *J. Cell Biol.* 145:1443–1460.

Manganas, L.N., S. Akhtar, D.E. Antonucci, C.R. Campomanes, J.O. Dolly, and J.S. Trimmer. 2001. Episodic ataxia type-1 mutations in the Kv1.1 potassium channel display distinct folding and intracellular trafficking properties. *J. Biol. Chem.* 276:49427–49434.

Martinez-Botas, J., J.B. Anderson, D. Tessier, A. Lapillonne, B.H. Chang, M.J. Quast, D. Gorenstein, K.H. Chen, and L. Chan. 2000. Absence of perilipin results in leanness and reverses obesity in Lepr(db/db) mice. *Nat. Genet.* 26:474–479.

McManaman, J.L., W. Zabaronick, J. Schaack, and D.J. Orlicky. 2003. Lipid droplet targeting domains of adipophilin. *J. Lipid Res.* 44:668–673.

Monné, M., I. Nilsson, A. Elofsson, and G. von Heijne. 1999. Turns in transmembrane helices: determination of the minimal length of a "helical hairpin" and derivation of a fine-grained turn propensity scale. *J. Mol. Biol.* 293:807–814.

Mora, R., V.L. Bonilha, A. Marmorstein, P.E. Scherer, D. Brown, M.P. Lisanti, and E. Rodriguez-Boulan. 1999. Caveolin-2 localizes to the Golgi complex but redistributes to plasma membrane, caveolae, and rafts when co-expressed with caveolin-1. *J. Biol. Chem.* 274:25708–25717.

Murphy, D.J. 2001. The biogenesis and functions of lipid bodies in animals, plants and microorganisms. *Prog. Lipid Res.* 40:325–438.

Naested, H., G.I. Frandsen, G.Y. Jauh, I. Hernandez-Pinzon, H.B. Nielsen, D.J. Murphy, J.C. Rogers, and J. Mundy. 2000. Caleosins: Ca^{2+}-binding proteins associated with lipid bodies. *Plant Mol. Biol.* 44:463–476.

Nakamura, N., and T. Fujimoto. 2003. Adipose differentiation-related protein has two independent domains for targeting to lipid droplets. *Biochem. Biophys. Res. Commun.* 306:333–338.

Ostermeyer, A.G., J.M. Paci, Y. Zeng, D.M. Lublin, S. Munro, and D.A. Brown. 2001. Accumulation of caveolin in the endoplasmic reticulum redirects the protein to lipid storage droplets. *J. Cell Biol.* 152:1071–1078.

Parolini, I., M. Sargiacomo, F. Galbiati, G. Rizzo, F. Grignani, J.A. Engelman, T. Okamoto, T. Ikezu, P.E. Scherer, R. Mora, et al. 1999. Expression of caveolin-1 is required for the transport of caveolin-2 to the plasma membrane. Retention of caveolin-2 at the level of the Golgi complex. *J. Biol. Chem.* 274: 25718–25725.

Pol, A., R. Luetterforst, M. Lindsay, S. Heino, E. Ikonen, and R.G. Parton. 2001. A caveolin dominant negative mutant associates with lipid bodies and induces intracellular cholesterol imbalance. *J. Cell Biol.* 152:1057–1070.

Sargiacomo, M., P.E. Scherer, Z.L. Tang, E. Kübler, K.S. Song, M.C. Sanders, and M.P. Lisanti. 1995. Oligomeric structure of caveolin: implications for caveolae membrane organization. *Proc. Natl. Acad. Sci. USA.* 92:9407–9411.

Schlegel, A., and M.P. Lisanti. 2000. A molecular dissection of caveolin-1 membrane attachment and oligomerization. Two separate regions of the caveolin-1 C-terminal domain mediate membrane binding and oligomer/oligomer interactions in vivo. *J. Biol. Chem.* 275:21605–21617.

Schlegel, A., R.B. Schwab, P.E. Scherer, and M.P. Lisanti. 1999. A role for the caveolin scaffolding domain in mediating the membrane attachment of caveolin-1. The caveolin scaffolding domain is both necessary and sufficient for membrane binding in vitro. *J. Biol. Chem.* 274:22660–22667.

Schroeder, R.J., S.N. Ahmed, Y. Zhu, E. London, and D.A. Brown. 1998. Cholesterol and sphingolipid enhance the Triton X-100-insolubility of GPI-anchored proteins by promoting the formation of detergent-insoluble ordered membrane domains. *J. Biol. Chem.* 273:1150–1157.

Smart, E.J., G.A. Graf, M.A. McNiven, W.C. Sessa, J.A. Engelman, P.E. Scherer, T. Okamoto, and M.P. Lisanti. 1999. Caveolins, liquid-ordered domains, and signal transduction. *Mol. Cell. Biol.* 19:7289–7304.

Tansey, J.T., C. Sztalryd, J. Gruia-Gray, D.L. Roush, J.V. Zee, O. Gavrilova, M.L. Reitman, C.-X. Deng, C. Li, A.R. Kimmel, and C. Londos. 2001. Perilipin ablation results in a lean mouse with aberrant adipocyte lipolysis, enhanced leptin production, and resistance to diet-induced obesity. *Proc. Natl. Acad. Sci. USA.* 98:6494–6499.

Tansey, J.T., A.M. Huml, R. Vogt, K.E. Davis, J.M. Jones, K.A. Fraser, D.L. Brasaemle, A.R. Kimmel, and C. Londos. 2003. Functional studies on native and mutated forms of perilipins. A role in protein kinase A-mediated lipolysis of triacylglycerols in Chinese hamster ovary cells. *J. Biol. Chem.* 278:8401–8406.

Targett-Adams, P., D. Chambers, S. Gledhill, R.G. Hope, J.F. Coy, A. Girod, and J. McLauchlan. 2003. Live cell analysis and targeting of the lipid droplet-binding adipocyte differentiation-related protein. *J. Biol. Chem.* 278:15998–16007.

Tzen, J.T., G.C. Lie, and A.H. Huang. 1992. Characterization of the charged components and their topology on the surface of plant seed oil bodies. *J. Biol. Chem.* 267:15626–15634.

Ward, T.H., R.S. Polishchuk, S. Caplan, K. Hirschberg, and J. Lippincott-Schwartz. 2001. Maintenance of Golgi structure and function depends on the integrity of ER export. *J. Cell Biol.* 155:557–570.

Zweytick, D., K. Athenstaedt, and G. Daum. 2000. Intracellular lipid particles of eukaryotic cells. *Biochim. Biophys. Acta.* 1469:101–120.

Downloaded from jcb.rupress.org on January 4, 2012